Commensurate Modulated Displacement and Disorder in the Mixed Valent Vanadium Monophosphate $Sr_2V_2O(PO_4)_3$

S. Boudin, O. Pérez, H. Leligny, D. Grebille,* Ph. Labbé, and B. Raveau

Lab. CRISMAT (UMR CNRS 6508), ISMRA, Bd du Maréchal Juin, 14050 Caen, Cedex, France

Received March 13, 1997[⊗]

A new mixed-valent monophosphate $Sr_2V_2O(PO_4)_3$ has been synthesized. Its 4-fold superstructure has been refined using the 4D formalism for modulated structures and using X-ray single-crystal diffraction data. The average structure can be described as a stacking of $[V_2P_3O_{13}]_\infty$ layers and $[Sr_2]_\infty$ layers. In these layers, the VO_6 octahedra, occupied by V(III), the VO_5 trigonal bipyramids, occupied by V(IV), and the PO_4 tetrahedra form chains running along **b**. The 4D description allows us to give a better description of the measured intensities in reciprocal space (main and first order satellite reflections) and particularly to explain why the second order satellite reflections are not observed using a classical X-ray source. The corresponding structural mechanism consists of an alternation of disordered ribbons of VO_5 bipyramids and PO_4 tetrahedra in two enantiomorphic configurations, separated by displacively modulated ribbons of VO_6 octahedra and PO_4 tetrahedra. Crystal data: monoclinic, superstructure space group $P2_1/c$, $Z = 8$, $a = 17.389(1)$ Å, $b = 5.094(1)$ Å, $c = 30.032(4)$ Å, $\beta = 132.17(1)°$; superspace group $P2_1/m(0,0,{}^1/_4)0s$, $Z = 2$, $c' = c/4$.

1. Introduction

The chemistry of transition metal phosphates with interpolated cations began in the 1970s. Before this, these materials appeared to be of great interest for their physical properties. For example, the Nasicon tunnel structure, $NaZr_2(PO_4)_3$, discovered by Hagman and Kierkegaard,[1] showed interesting ionic conduction properties, whereas the nonlinear optical phosphate, $KTiOPO_4$, was known for its second harmonic generation properties.[2] Some years later, the A−M−P−O compounds with M = Ti, Nb, W, Mo, and V were widely investigated. More recently, numerous transition metal phosphates such as those of tungsten[3] and those of molybdenum[4] have been discovered.

The investigation of vanadium phosphates started six years ago and has allowed several new reduced vanadium phosphates to be isolated. Among them, the Sr−V−P−O compounds are of interest, although they are rather rare. In these strontium vanadium phosphates, vanadium is present in various oxidation states. Various structures are found such as for the V(III) phosphates $Sr_2V(PO_4)_2(H_2PO_4)$[5] or $SrV_2(P_2O_7)_2$[6] and $SrV_2O(PO_4)_2$[7] that are either unidimensional or tridimensional. The V(IV) phosphate $Sr(VO_2)(PO_4)_2{\cdot}4H_2O$[8] and the V(V) phosphate $Sr(VO_2)(PO_4)$[9] are bidimensional.

All the strontium vanadophosphates synthesized to date are built up of VO_6 octahedra and PO_4 tetrahedra, but none of them exhibit mixed vanadium valence, in contrast to the molybdenum or tungsten phosphates. In the present study, we report on the layer structure of a new monophosphate, $Sr_2V_2O(PO_4)_3$, that exhibits mixed-valence V(III)−V(IV) and contains both VO_6 octahedra and VO_5 trigonal bipyramids.

The originality of this new phase concerns its 4-fold superstructure, which can be interpreted as a commensurate modulated structure. The present structure determination was performed using four-dimensional formalism for the modulated phases.[10]

2. Experimental Section

2.1. Synthesis. The synthesis was performed in two steps. Firstly, $SrCO_3$, V_2O_5, and $H(NH_4)_2(PO_4)_2$ were mixed and heated at 893 K for 2 h to obtain an intermediate mixture with composition $SrV^V_{1.6}P_2O_{10}$. Secondly, the appropriate amount of V and 10% NaCl in weight ratio were added to obtain a sample of nominal composition $SrV_2PO_2O_{10}$, 10% NaCl. This mixture was placed in an alumina crucible, sealed in an evacuated silica ampule, and heated at 1173 K for 24 h, slowly cooled to 973 K at a rate of 2 $K{\cdot}hr^{-1}$, and quenched to room temperature. Single crystals of $Sr_2V_2O(PO_4)_3$ were then extracted from the sample.

Polycrystalline samples of $Sr_2V_2O(PO_4)_3$ were also prepared with a similar synthesis procedure. However, the intermediate mixture composition was $Sr_2V^V_{1.4}P_3O_{13}$ and only metallic vanadium was added at the second step to obtain the composition $Sr_2V_2P_3O_{13}$. The silica ampule was heated at 1373 K for 24 h and quenched to room temperature.

2.2. Data Collection. A brown lamellar crystal of dimensions 0.051 × 0.141 × 0.026 mm^3 was selected for the structure determination. Preliminary Weissenberg camera photographs confirmed the crystalline quality of the sample and did not show any diffuse scattering. They showed monoclinic symmetry and a systematic extinction of the (*hkl*) reflections with $l = 4n + 2$. X-ray intensity data were recorded at room temperature on a CAD4 Enraf-Nonius diffractometer using Mo Kα radiation up to $\theta = 45°$. Unfortunately, only 1131 reflections had a significant value ($I \geq 3\sigma(I)$), with a lot of unmeasured reflections with too weak intensity. A satisfactory structure refinement was not possible using this first data collection. In spite of the unfavorable value of the linear absorption coefficient (μ(Cu) = 370 cm^{-1} instead of μ(Mo) = 138 cm^{-1}), the intensities were measured using monochromated Cu Kα radiation up to $\theta = 75°$, resulting in 1914 significant values (Table 1). The cell parameters $a = 17.389(1)$ Å, $b = 5.094(1)$

[⊗] Abstract published in *Advance ACS Abstracts,* September 1, 1997.

(1) Hagman, L. O.; Kierkegaard, P. *Acta. Chem. Scand.* **1968**, *22*, 1822.
(2) Zumsteg, F. C.; Bierlein, J. D.; Gier, T. E. *J. Appl. Phys.* **1976**, *47*, 4980.
(3) Borel, M. M.; Goreaud, M.; Grandin, A.; Labbé, Ph.; Leclaire, A.; Raveau, B. *Eur. J. Solid State Inorg. Chem.* **1991**, *28*, 93.
(4) Costentin, G.; Leclaire, A.; Borel, M. M.; Grandin, A.; Raveau, B. *Rev. Inorg. Chem.* **1993**, *13*, 77.
(5) Lii, K. H.; Lee, T. C.; Liu, S. N.; Wang, S. L. *J. Dalton Trans., Inorg. Chem.* **1993**, 1051.
(6) Hwu, S. J.; Willis, E. D. *J. Solid State Chem.* **1991**, *93*, 69.
(7) Boudin, S.; Grandin, A.; Labbé, Ph.; Provost, J.; Raveau, B. To be published.
(8) Kang, H. Y.; Lee, W. C.; Wang, S. L. *Inorg. Chem.* **1992**, *31*, 4743.
(9) Wang, K.; Lii, K. H. *Acta Crystallogr.* **1992**, *C48*, 975.
(10) Wilson, A. J. C. *International Tables for Crystallography*; Kluwer Academic Publishers: Dordrecht, 1992; Vol. C, pp 384.

S0020-1669(97)00285-1 CCC: $14.00

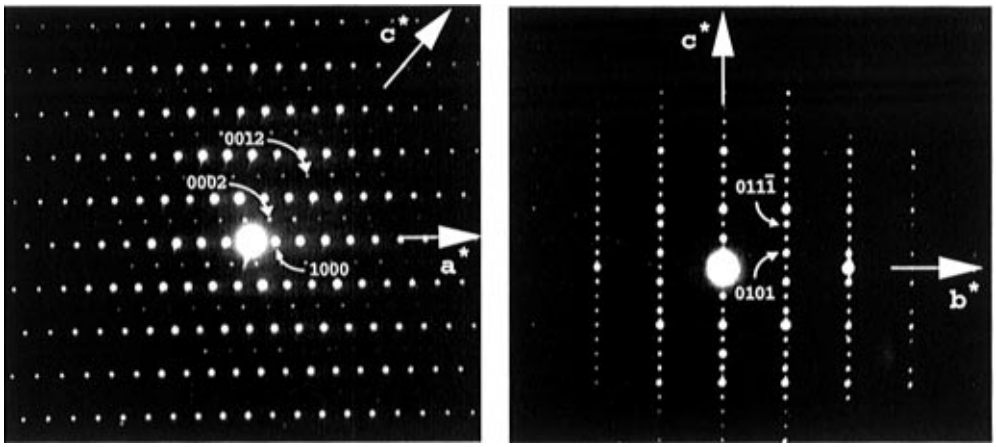

Figure 1. Electron diffraction pattern of $Sr_2V(VO)(PO_4)_3$: (a, left) [010] zone axis showing the absence of first-order satellites and weak second-order satellites in the (*h*0*l*) layer; (b, right) [100] zone axis.

Table 1. Crystallographic Data

formula	$Sr_2V(VO)(PO_4)_3$
fw	578
T, K	293
cryst syst	monoclinic
superspace group	$P2_1/m(0,0,^1/_4)0s$
a, Å	17.389(1)
b, Å	5.094(1)
c, Å	4 × 7.508(1)
β, deg	132.17(1)
V, Å^3	492.9(1)
Z	2
ρ_{calcd}, g cm^{-3}	3.90
λ, Å	1.5418
μ, cm^{-1}	370
$R(F_o)$,[a] $R_w(F_o)$[b]	0.063, 0.066
$R_0(F_o)$,[a] $R_{w0}(F_o)$[b]	0.054, 0.060
$R_1(F_o)$,[a] $R_{w1}(F_o)$[b]	0.076, 0.077

[a] $R = \sum||F_o| - |F_c||/\sum|F_o|$. [b] $R_w = (\sum w(|F_o| - |F_c|)^2/\sum|F_o|^2)^{1/2}$. *R*, R_0, and R_1 are related to the agreement factors for all, main, and satellite reflections, respectively.

Å, *c* = 30.032(4) Å, and β = 132.17(1)° were refined using 25 reflections with 18° < θ < 22°. No significant variation of the intensity of three standard reflections measured every 50 min was detected. Data sets were corrected for Lorentz and polarization effects. An analytical absorption correction was performed, based on an accurate determination of the morphology and of the size of the crystal, using the JANA package.[11]

2.3. Electron Microscopy Study. Powders of the same batch as the X-ray studied single crystal were gently ground in an agate mortar in 1-butanol and deposited on a holey carbon coated copper grid. Electron diffraction (ED) was performed on a JEM200CX equipped with a tilting rotating goniometer (±60°), which allows reconstruction of the reciprocal space.

2.4. Magnetic Measurements. Magnetic moments of powdered samples were measured from 42 to 300 K with a SQUID magnetometer. The 10 000 G field was applied after cooling at 4.5 K. The molar susceptibility χ_m was extracted after correction of the sample holder signal and of the core diamagnetism of all of the atoms.

$Sr_2V_2O(PO_4)_3$ is paramagnetic and follows the Curie−Weiss law with the Curie constant $\Theta = -8K$ and C_m = 1.36 emu·K/mol corresponding to an effective magnetic moment of 2.36 μ_B for $0.5V^{III} + 0.5V^{IV}$ ions.

3. Diffraction Pattern and Symmetry

Both the Weissenberg camera photographs and the measured diffracted intensities show unusual features. In the (*h*0*l*) layer, only the *l* = 4*n* lattice rows are observed, and in the general (*hkl*) layers, the *l* = 2(2*n* + 1) rows are systematically absent. One also observes that the reflections (*hkl*) with *l* = 4*n* are generally more intense than the reflections (*hkl*) with *l* = 4*n* ± 1. Moreover, the reflection condition *k* = 2*n* for the (0*k*0) reflections is also observed. These X-ray diffraction results can be compared and confirmed with electron diffraction observations (Figure 1). However, one also observes (*hkl*) reflections with *l* = 2(2*n* + 1), but they are much weaker, and this very low intensity explains why they are not measurable by classical X-ray diffraction techniques. These features are generally compatible with monoclinic symmetry $P2_1/c$, but they cannot be completely explained in the framework of a standard monoclinic symmetry.

Another interpretation can be given for the diffraction pattern: if we consider the more intense reflections (*hkl*) with *l* = 4*n* as main reflections, and the others as superstructure reflections, the structure can be described as a commensurate modulated structure with a basic cell $\mathbf{a}' = \mathbf{a}$, $\mathbf{b}' = \mathbf{b}$, and $\mathbf{c}' = \mathbf{c}/4$. The weaker superstructure reflections can be considered as satellite reflections characterized by a modulation wavevector $\mathbf{q}^* = \gamma\mathbf{c}'^*$ with a rational component $\gamma = {}^1/_4$. In the new reciprocal lattice, one can now distinguish between main and satellite reflections which can be written by four indices *h*′, *k*′, *l*′, and *m*′ (with *h* = *h*′, *k* = *k*′, and *l* = 4*l*′ + *m*′). Taking into account the previous extinction conditions, one can conclude that second-order satellites are too weak to be measured by X-ray diffraction, and this observation is still to be explained.

In the new lattice, there is no general extinction rule concerning the reflections (*h*′*k*′*l*′*m*′). The supercrystal lattice is primitive, and the Bravais class is $P2/m(\alpha 0\gamma)$[10] with $\alpha = 0$ and $\gamma = {}^1/_4$. The observed reflection conditions are (0*k*′00), *k*′ = 2*n*, and (*h*′0*l*′*m*′), *m*′ = 2*n*, involving the symmetry operators $\begin{pmatrix}2_1\\ \bar{1}\end{pmatrix}$ and $\begin{pmatrix}m\\ s\end{pmatrix}$, respectively. The superspace group (SSG) is $P2_1/m(\alpha 0\gamma)0s$ (unique axis **b**), equivalent to the standard SSG: $P2_1/m(\alpha\beta 0)0s$ (unique axis **c**). This symmetry does not explain the apparent extinction observed for the second order satellite reflections. These reflections should probably be observed with a more intense X-ray source. However, an explanation will be given further for their particularly weak intensity.

The electron diffraction study confirmed the reflection conditions established by XRD. The *h*′0*l*′2 reflections are clearly visible by electron diffraction (Figure 1), although they appear much weaker than the main reflections (*m*′ = 0). Furthermore, no systematic extinction is observed in the 0*k*′*l*′*m*′ pattern, and the presence of 00*l*′*m*′, *m*′ = 2*n* + 1, and 0*k*′00, *k*′ = 2*n* + 1 reflections is probably due to double diffraction phenomena.

Considering the commensurate character of the modulation, we know that the crystal in real space is a particular section of

(11) Petricek, V. *Crystallographic computing system JANA94*; Institute of Physics, Academy of Sciences of the Czech Republik: Prague, 1994.

the four-dimensional supercrystal. Since superspace-group elements result in three-dimensional symmetry in a given section t,[12] two different kinds of sections occur in the present case: the general sections $t \neq n/8$, of symmetry Pc, and the particular sections $t = n/8$, for which all the symmetry operators of the supercrystal also belong to the real space section. These latter sections are compatible with a global three-dimensional symmetry $P2_1/c$. They are all equivalent and are compatible with the observed reflection conditions in the supercell. This symmetry hypothesis ($t = 0$) is considered for the refinement.

4. Structure Refinement

The average structure was first determined using direct methods with the Xtal3.2 package.[13] The refinement was performed in the subcell $\mathbf{a}'$, $\mathbf{b}'$, $\mathbf{c}'$ in space group $P2_1/m$ using only the main reflections ($m' = 0$). Except for three oxygen atoms in general positions, all the atoms were first located in special positions (2e) on the mirror plane m. Because of abnormally high values for the thermal B_{22} component, some atoms split over two disordered positions on each side of the mirror plane. The final R factor using $|F|$ is 0.105. Most of the thermal parameters were still too large along $\mathbf{b}$. As it was not reasonable to imagine that most of the atoms were disordered over two sites, and as the refinement in the supercell involves too many parameters, a refinement was tried using a commensurately modulated structure with the program JANA94.[11] A unit weight was chosen for all reflections in order to improve the refinement of the modulation functions from the weaker intensities of the first-order satellites. Refinement was carried out in the section $t = 0$. A trial refinement in a general section did not significantly improve the results.

Both occupational and displacive modulations, P^μ and $\mathbf{U}^\mu$, can be considered for the atom μ. They are described with their Fourier expansion as a function of the internal coordinate $x_4^\mu = \mathbf{q}^*\cdot\mathbf{r}_0^\mu + \varphi = \gamma z_0^\mu + \varphi$, where $\mathbf{r}_0^\mu$ is the average position of the atom μ in the subcell and where $\varphi = \mathbf{q}^*\cdot\mathbf{p} = \gamma n_3 = n_3/4$ describes the internal phase corresponding to the cell $\mathbf{p} = n_1\mathbf{a}' + n_2\mathbf{b}' + n_3\mathbf{c}'$. As a consequence of the rational value of γ, φ takes only the value 0, $^1/_4$, $^1/_2$, and $^3/_4$. The corresponding modulation functions can be written

$$P^\mu(\bar{x}_4^\mu) = \overline{P^\mu} + A^\mu \cos(2\pi\bar{x}_4^\mu) + B^\mu \sin(2\pi\bar{x}_4^\mu)$$

$$U_i^\mu(\bar{x}_4^\mu) = A_i^\mu \cos(2\pi\bar{x}_4^\mu) + B_i^\mu \sin(2\pi\bar{x}_4^\mu), \quad i = 1, 2, 3$$

Since the second-order satellites have not been observed, only the first-order harmonic has been considered.

Large thermal parameters in the average structure can be interpreted in two different ways: they result either from a modulated displacement around the average position or from positional disorder. For an atom μ in special position (2e) in the average structure, these two hypotheses lead to two very different configurations.

In the first case, the average position is still a special position and symmetry restrictions must be considered for the atom μ, resulting from the action of the symmetry operator $\begin{pmatrix} m \\ s \end{pmatrix}$ onto the modulation functions. It is found that $U_i^\mu = 0$ for $i = 1, 3$ and $A^\mu = B^\mu = 0$. In this case, only a transverse modulated displacement U_2^μ is allowed and the site occupation is constant. In the second case, the atom is in general position (4f) and there are two equivalent sites μ and ν with an average occupation

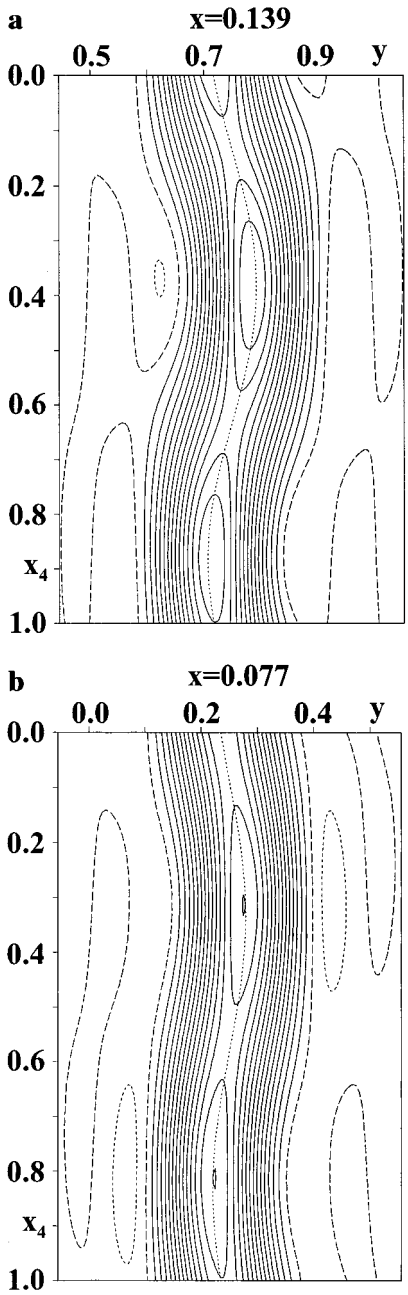

Figure 2. Sections $x_2 - x_4$ of the four-dimensional difference Fourier maps corresponding to the displacively modulated atoms: (a) Sr(2) and (b) P(2).

0.5 on each side of the mirror plane. The modulation functions of the two sites are dependent and related through $A^\mu = -A^\nu$ and $B^\mu = -B^\nu$, so that $P^\mu + P^\nu = 2\overline{P^\mu} = 1$.

In the first instance, only displacive modulations were taken into account for all atoms in special positions (2e) (i.e., all atoms except O(9) and O(10)). As a result, the 4D-Fourier density maps clearly showed two types of behaviors: the atom is represented either by a continuous string along the internal direction (see, for example, atom Sr(2) or P(2), Figure 2) or by a discontinuous pattern with two individualized maxima on each side of the mirror plane for $x_4 = 0.2$ or $x_4 = 0.7$ (see, for example, Sr(1) or P(3), Figure 3). These two types of behaviors can be directly related to the two previous configurations (displacive modulation or disorder). Secondly, therefore, the atoms were considered to be either displacively modulated in special position (Sr(2), V(1), P(1), P(2), all oxygen atoms except O(8), O(11)) or occupationally modulated in general position without any displacement parameter at this step (Sr(1), V(2), P(3), O(8), O(11)). Finally, in a third step, a displacive

(12) Dam, B.; Janner, A. *Acta Crystallogr.* **1986**, *B42*, 69.
(13) Hall, S. R.; King, G. S. D.; Stewart, J. M. *Xtal3.2 System of Crystallographic Programs*; University of Western Australia: Lamb, Perth, 1993.

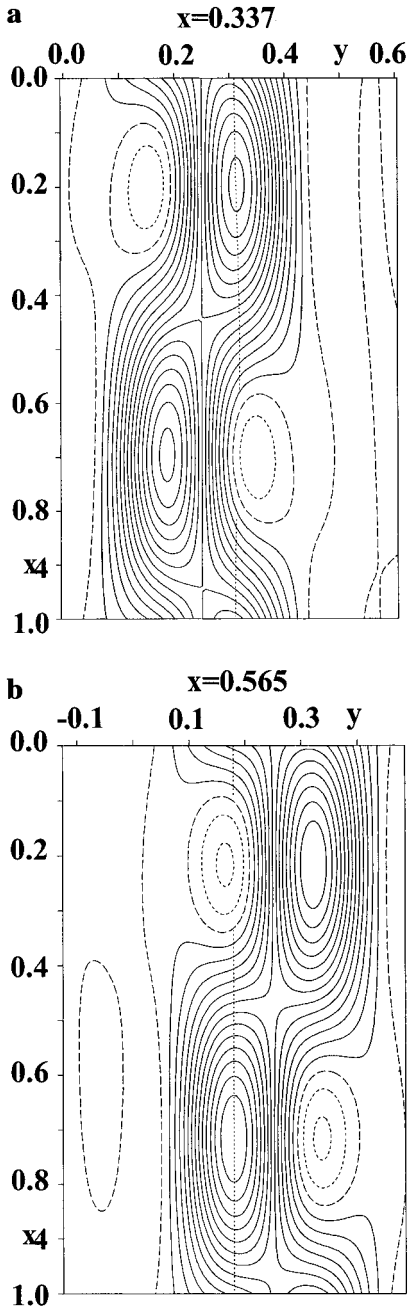

Figure 3. Sections $x_2 - x_4$ of the four-dimensional difference Fourier maps corresponding to the occupation modulated atoms: (a) Sr(1) and (b) P(3).

modulation was also taken into account for the disordered sites. Some corresponding parameters are significant; others are small and, consequently were fixed to 0. The oxygen atoms O(9) and O(10) are in general position and were considered as being displacively modulated. Sr, V, and P were given anisotropic thermal parameters; O was refined with isotropic parameters. The global R and R_w factors are 0.063 and 0.066, respectively (0.054 and 0.060 for main reflections, 0.076 and 0.077 for first-order satellites). The results are summarized in Table 2.

5. Discussion

5.1. The Modulation Structural Features. The most notable and unexpected property of the crystal is the existence of split sites, which are related by the mirror plane m for the Sr(1), V(2), P(3), O(8), and O(11) atoms. In the following discussion, these pairs of sites will be denoted + and −, where the symbol + stands for the site at a distance δb away from the mirror plane with $\delta > 0$. The distances between two corresponding split sites are rather large: 0.64, 1.21, 0.72, 1.53, and 1.63 Å. As indicated from the analysis of the electron density maps from the results of the refinement of the corresponding displacive parameters, these split sites are very weakly affected by the displacive modulation. Since the modulation is commensurate, only four values for the occupancy of each site in a pair of split sites in the section $t = 0$ are actually relevant. Values very close to 0, $^1/_2$, and 1 are observed on each site, within experimental error, although they were not imposed by symmetry. Values slightly below 0 or above 1 are probably due to truncature effects in the Fourier expansions. It is thus verified that, for the Sr(1), V(2), P(3), O(8), and O(11) atoms, each atom occupies only one of the two available sites in the unit cells $n_3 = 4n$ (+ or −) and $n_3 = 4n + 2$ (− or +) (Figure 4). In these cells, the existence of two disordered sites is masked by the fact that the probability of occupation is 0 for the opposite site; the corresponding sites will be labeled V(2)a and P(3)a. In the other cells, the two sites + and − are occupied with the same probability, $^1/_2$, and a real disorder occurs; this will be denoted by ±; and the corresponding sites will be labeled V(2)b and P(3)b. The occupancy sequence (+, ±, −, ±) is consistent with the supercell symmetry $P2_1/c$. Moreover, in each subcell, in correspondence with a given pair of sites of the primary sequence (+, ±, −, and ±), a second pair of sites is generated by the 4D symmetry operation $\begin{pmatrix} 2_1 \\ \bar{1} \end{pmatrix}$ giving respective occupation probabilities ±, +, ±, and −. These sequences are illustrated in Figure 4.

The other atoms are characterized by a displacive modulation. Most of these atoms sit on a special position m in the average structure, and the displacements appear along **b′** (transverse modulation). Larger amplitudes (about 0.4 Å) are observed for the oxygen atoms O(5), O(6), and O(7); whereas smaller amplitudes (about 0.2 Å) are observed for Sr(2), V(1), P(1), and P(2). The atoms O(9) and O(10), which occupy general positions in the average structure, show, in addition to the displacement along **b′**, small but significant displacements along **a′** and **c′** (less than 0.2 Å).

5.2. The Interatomic Bond Scheme. The bond lengths related to the atomic pairs Sr−O, V−O, and P−O are shown in Table 3. The different hypotheses involving disorder have to be carefully scrutinized for these distance calculations. Looking at all the different structural possibilities, some arrangements lead to too short bond lengths or to unreasonable chemical environments and, thus, can be discarded. For example, P(3) is bonded to O(8) and O(11) and the only possible configurations which correspond to the usual tetrahedral coordination of phosphorus are +, −, − or −, +, + for these three atoms, respectively. Similarly, V(2) is also bonded to O(8) and O(11) and the only acceptable local configurations are also +, −, − or −, +, +. From these considerations, it can be concluded that there is a complete correlation between the local site occupancies of V(2), P(3), O(8), and O(11) sites. These atoms can, thus, be considered as building one unique block with only two different configurations which will be denoted + or −, following on from the type of site occupancy of the cations V(2) and P(3).

Only two distinct types of oxygen environments are implied for the Sr(2), V(1), P(1), and P(2) atoms, corresponding to the $n_3 = 2n$ and n_3 and $2n + 1$ cells, respectively. Three types of environments have to be considered for the V(2) and P(3) atoms. In fact, V(2) and P(3) may occupy either the + or the − sites in the unit cells defined by $n_3 = 4n \pm 1$. Some O atoms of the related coordination polyhedra are affected by the displacive

Table 2. Atomic Positional, Occupational, and Equivalent Isotropic Thermal Parameters[a]

		A_0	A_1	B_1
Sr(1)	U_1	0.3371(1)	0.0021(2)	0*
	U_2	0.3141(4)	−0.006(1)	0*
	U_3	0.7652(2)	0.0035(5)	0*
	P	0.5	0.22(1)	0.61(2)
	U_{eq}, Å^2	0.0180		
Sr(2)	U_1	0.1386(1)		
	U_2	0.75	−0.0332(8)	0.031(1)
	U_3	0.6998(2)		
	U_{eq}, Å^2	0.0199		
V(1)	U_1	0.1562(2)		
	U_2	0.75	−0.016(1)	0.022(1)
	U_3	0.2170(3)		
	U_{eq}, Å^2	0.0155		
V(2)	U_1	0.4136(3)	0*	−0.044(3)
	U_2	0.626(1)	−0.016(2)	0*
	U_3	0.5526(4)	0*	0*
	P	0.5	−0.42(1)	−0.49(1)
	U_{eq}, Å^2	0.0149		
P(1)	U_1	0.2392(2)		
	U_2	0.25	−0.036(2)	0.016(1)
	U_3	0.1058(5)		
	U_{eq}, Å^2	0.0175		
P(2)	U_1	0.778(2)		
	U_2	0.25	−0.015(2)	0.027(2)
	U_3	0.3185(5)		
	U_{eq}, Å^2	0.0157		
P(3)	U_1	0.5651(2)	0*	0*
	U_2	0.1807(8)	0*	0*
	U_3	0.8479(5)	0*	0*
	P	0.5	−0.15(1)	−0.64(2)
O(1)	U_1	0.0402(6)		
	U_2	0.25	−0.003(3)	−0.011(3)
	U_3	0.449(2)		
	U_{iso}, Å^2	0.019		
O(2)	U_1	0.4287(6)		
	U_2	0.75	0.003(2)	−0.013(2)
	U_3	0.339(2)		
	U_{iso}, Å^2	0.021		
O(3)	U_1	0.0069(6)		
	U_2	0.75	−0.003(2)	0.035(3)
	U_3	0.950(2)		
	U_{iso}, Å^2	0.017		
O(4)	U_1	0.3172(6)		
	U_2	0.75	−0.018(3)	0.004(3)
	U_3	0.507(2)		
	U_{iso}, Å^2	0.020		
O(5)	U_1	0.2568(6)		
	U_2	0.25	0.005(2)	0.069(3)
	U_3	0.937(2)		
	U_{iso}, Å^2	0.017		
O(6)	U_1	0.3396(6)		
	U_2	0.25	−0.070(3)	−0.038(3)
	U_3	0.371(2)		
	U_{iso}, Å^2	0.020		
O(7)	U_1	0.3318(6)		
	U_2	0.75	0.015(3)	0.079(3)
	U_3	0.897(2)		
	U_{iso}, Å^2	0.016		
O(8)	U_1	0.5058(6)	0*	0*
	U_2	0.607(2)	0*	0*
	U_3	0.17(2)	0*	0*
	P	0.5	−0.18(2)	0.70(3)
	U_{iso}, Å^2	0.021		
O(9)	U_1	0.1511(4)	−0.003(1)	0.006(1)
	U_2	0.012(2)	−0.023(2)	0.040(2)
	U_3	0.407(1)	−0.001(2)	−0.007(2)
	U_{iso}, Å^2	0.018		
O(10)	U_1	0.1766(4)	−0.007(1)	0.004(1)
	U_2	0.009(2)	−0.034(2)	0.005(2)
	U_3	0.0556(9)	−0.027(2)	0.012(2)
	U_{iso}, Å^2	0.020		
O(11)	U_1	0.5166(6)	0*	0*
	U_2	0.593(2)	0*	0*
	U_3	0.795(2)	0*	0*
	P	0.5	0.20(2)	0.61(3)
	U_{iso}, Å^2	0.020		

[a] Parameters with asterisks (∗) were fixed during the refinement because they were not significant. A_0 is the average value of the modulation function, and A_1 and B_1 are the amplitudes of the cos and sin terms of the first-order Fourier term of the modulation function.

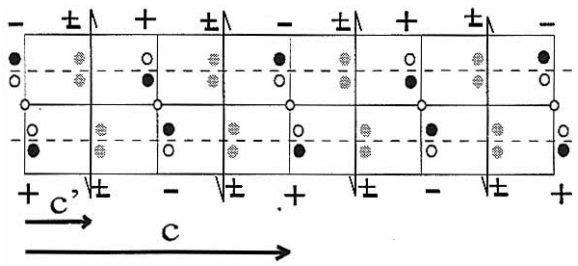

Figure 4. Schematic representation of one typical disordered site (Sr(1), V(2), P(3), O(8), or O(11)): open circles, full occupation; filled circles, zero occupation; gray circles, occupation $^1/_2$. The symmetry operators belong to the supercell ($P2_1/c$). In each subcell, one observes two different sites, symmetry related by the 4D screw axis (not represented).

modulations. The concept of bond valence[14] was used to verify both the coordination of the Sr atoms and the valence state of the V atoms. If we consider the two independent oxygen environments of Sr(2), 10 Sr−O distances ranging from 2.5 to 3.2 Å are observed (Table 3). Such 10-fold coordination leads to a bond valence sum very close to 2. Similar coordination is likely for the Sr atoms on the Sr(1) split sites (Table 3). In the unit cells defined by $n_3 = 2n$, only one environment has to be considered and leads to a valence sum of 1.97, since one of the disordered sites is fully occupied. In the unit cells defined by $n_3 = 4n \pm 1$, if we consider the different possible occupations of the O(8) and O(11) sites in the Sr(1) environment and their correlations, four possible coordinations can be deduced for Sr(1) (Table 3). The bond valence sums give rather high but acceptable values: between 2.06 and 2.26 for the + configuration, and between 1.92 and 2.31 for the − configuration (Table 3).

The chemical formula $Sr_2V_2O(PO_4)_3$ implies an average value of 3.5 for the vanadium valence, suggesting two distinct valence states on the V(1) and V(2) sites. This result is also in agreement with the previously described magnetic measurements. On the V(1) sites, the V atom exhibits octahedral coordination, with the V(1)−O distances ranging from 1.94 to 2.10 Å in the two independent polyhedra (Table 3). Its valence state is equal to 3, in agreement with the bond valence sums of 3.01 and 3.00 calculated for the two possible sites. On the V(2) site, the vanadium has 5-fold coordination; the V(2)−O distances show a noticeable dispersion from 1.56 to 2.21 Å, particularly in the third type of polyhedron. The corresponding polyhedra are distorted trigonal bipyramids. The valence state of vanadium is equal to 4, which corresponds to bond valence values of 4.01, 4.18, and 3.71 for the three possible environments of this disordered site.

5.3. The Structural Arrangement of the Modulated Crystal. The structure of this new strontium vanadophosphate (Figure 5) consists of $[V_2P_3O_{13}]_\infty$ layers paralled to $(10\bar{1})$, interleaved with $[Sr_2]_\infty$ layers. Each $[V_2P_3O_{13}]_\infty$ layer is made up of corner-sharing VO_5 trigonal bipyramids, VO_6 octahedra, and PO_4 tetrahedra, as shown on the projections of such a layer along [010] and [102] (Figure 6). In those layers, the V(1) octahedra and the P(1) and P(2) tetrahedra form $[VP_2O_8]_\infty$ chains running along **b**; two adjacent chains, related either by a 2-fold screw axis or by an inversion center, share some apices of their polyhedra forming double chains $[V_2P_4O_{16}]_\infty$, labeled A (Figure 6). The V(2) trigonal bipyramids, occupied by V(IV), and P(3) tetrahedra also form $[VPO_5]_\infty$ chains running along **b**; two such adjacent chains, related through the 4D symmetry operator $\left(\frac{2_1}{\bar{1}}\right)$, share corners, thus forming double chains $[V_2P_2O_{10}]_\infty$, labeled B (Figure 6).

(14) Brese, N. E.; O'Keeffe, M. *Acta Crystallogr.* **1991**, *B47*, 192.

Table 3. Selected Bond Lengths Calculated for the Atomic Pairs Sr−O, V−O, and P−O in the Basic Unit Cells $n_3 = 2n$ and $n_3 = 2n + 1$[a]

		$n_3 = 2n$	$n_3 = 2n + 1$
Sr(2)	O(1)	3.036(4)	3.162(4)
	O(1)^{i}	2.841(4)	2.720(4)
	O(1)^{ii}	2.50(2)	2.51(2)
	O(5)	2.750(5)	3.174(5)
	O(5)^{i}	3.244(5)	2.817(5)
	O(7)	2.63(2)	2.62(2)
	O(9)^{i}	2.74(1)	2.82(1)
	O(9)^{iii}	2.67(1)	2.60(1)
	O(10)^{iv}	2.52(1)	2.74(1)
	O(10)^{v}	2.75(1)	2.54(1)
$\sum$s		1.99	2.00
V(1)	O(3)^{vi}	1.94(1)	1.94(1)
	O(4)	2.10(1)	2.10(1)
	O(9)^{i}	2.00(1)	1.99(1)
	O(9)^{iii}	1.99(1)	2.02(1)
	O(10)^{i}	1.99(1)	2.03(1)
	O(10)^{iii}	1.99(1)	1.94(1)
	$\sum$s	3.01	3.00
P(1)	O(5)^{vi}	1.50(2)	1.51(2)
	O(6)	1.55(1)	1.53(1)
	O(10)	1.53(1)	1.53(1)
	O(10)^{iiii}	1.50(1)	1.51(1)
P(2)	O(1)	1.50(2)	1.51(2)
	O(3)^{ii}	1.50(1)	1.50(1)
	O(9)	1.55(1)	1.55(1)
	O(9)^{iii}	1.55(1)	1.56(1)

		$n_3 = 2n$	$n_3 = 2n + 1$	$n_3 = 2n + 1$
$\bar{y}$(Sr(1))		0.3141	0.3141	0.1859
Sr(1)	O(4)	2.78(1)	2.84(1)	2.77(1)
	O(5)	2.45(2)	2.47(2)	2.48(2)
	O(6)	3.07(2)	3.00(2)	3.01(2)
	O(7)^{vii}	2.67(1)	3.10(1)	3.02(1)
	O(7)	2.85(1)	2.42(1)	2.49(1)
	O(8)^{v}		3.28(1)^{a_1}	2.85(1)^{a_1}
	O(8)^{viii}	2.85(1)	2.86(1)^{a_2}	3.20(1)^{a_2}
	O(8)^{ix}		2.49(2)^{b_1}	2.63(2)^{b_1}
	O(8)^{x}	2.65(2)	2.69(2)^{b_2}	2.46(2)^{b_1}
	O(9)	2.87(1)	2.72(1)	3.08(1)
	O(9)^{iii}	2.64(1)	2.72(1)	2.51(1)
	O(11)^{xi}		2.53(1)^{a_1}	2.68(1)^{a_1}
	O(11)^{xii}	2.70(1)	2.74(1)^{a_1}	2.50(1)^{a_2}
$\sum$s		1.97	2.26$^{a_1-b_1}$, 2.06$^{a_2-b_2}$	2.12$^{a_1-b_1}$, 2.31$^{a_2-b_2}$
			2.11$^{a_1-b_2}$, 2.21$^{a_2-b_1}$	2.26$^{a_1-b_2}$, 1.92$^{a_2-b_2}$
$\bar{y}$(V(2))		0.626	0.626	0.874
V(2)	O(2)	1.85(2)	1.90(2)	1.91(2)
	O(4)	1.65(2)	1.56(2)	1.64(2)
	O(6)	1.91(1)	2.21(1)	2.18(1)
	O(8)^{ix}	1.96(1)	1.97(1)	
	O(8)^{xiv}			1.90(1)
	O(11)^{xiii}	1.99(1)	2.02(1)	
	O(11)			2.08(1)
$\sum$s		4.18	4.01	3.71
$\bar{y}$(P(3))		0.1807	0.1807	0.3193
P(3)	O(2)^{ix}	1.532(6)	1.511(6)	1.520(6)
	O(7)^{xi}	1.506(3)	1.548(3)	1.543(3)
	O(8)^{ix}	1.57(2)	1.57(2)	
	O(8)^{x}			1.57(2)
	O(11)^{iii}	1.54(2)	1.54(2)	
	O(11)			1.54(2)

[a] One observes two types of environments for the nondisordered sites Sr(2), V(1), P(1), and P(2), three for the totally correlated disordered sites V(2) and P(3), and nine for Sr(1) ((a_1, a_2), and (b_1, b_2) correspond to two pairs of possible exclusive configurations). The sum $\sum s$ of the bond valences is calculated for the pairs Sr−O and V−O. Symmetry codes: (i) x, $1 + y$, z; (ii) $-x$, $1 - y$, $1 - z$; (iii) x, $^1/_2 - y$, z; (iv) x, $1 + y$, $1 + z$; (v) x, $^1/_2 - y$, $1 + z$; (vi) x, y, $-1 + z$; (vii) x, $-1 + y$, z; (viii) x, y, $1 + z$; (ix) $1 - x$, $1 - y$, $1 - z$; (x) $1 - x$, $-^1/_2 + y$, $1 - z$; (xi) $1 - x$, $1 - y$, $2 - z$; (xii)$1 - x$, $-^1/_2 + y$, $2 - z$; (xiii) x, $^3/_2 - y$, z; (xiv) $1 - x$, $^1/_2 + y$, $1 - z$.

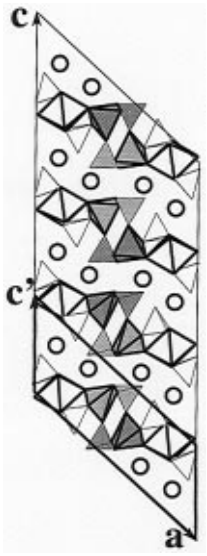

Figure 5. Schematic representation of the $Sr_2V_2O(PO_4)_3$ structure in the supercell, showing the stacking of $[V_2P_3O_{13}]_\infty$ and $[Sr_2]_\infty$ slices: blank polyhedra, displacively modulated coordination polyhedra of V(1), P(1), and P(2); gray polyhedra, disordered coordination polyhedra of V(2) and P(3); bright gray, full occupation (+ or −, see text); dark gray, disordered sites with occupation $^1/_2$. Only the − configuration has been represented.

The sequence of the modulated displacements of the ordered sites and of the occupancies of the disordered sites in the direction [101] of a layer can easily be deduced from the atomic sequences described in the previous section.

Each double chain, A, is perfectly ordered, but owing to the displacive modulation, two types of chains can be differentiated. In the first type (labeled A0 in Figure 6), the O(6) atom is very close to its average position and the two individual chains of the double chain are related by a 2-fold screw axis; in the second type (labeled A1), the modulated displacement of the O(6) atom is at a maximum and the chain is characterized by the presence of inversion centers.

In contrast to the A double chains, the B double chains exhibit an important disorder on the V(2) and P(3) sites. As deduced from the calculation of the V(2)−O and P(3)−O bond lengths, these disordered neighboring sites are fully correlated with the O atoms. This correlation means that the $[VPO_5]_\infty$ chains are characterized by a half-occupation of the disordered atomic sites, leading to two possible configurations instead of four, assuming a completely random occupation of the cationic sites. These two configurations are, in fact, enantiomorphic (Figure 7). Inside each B double chain, both split (±) and single sites (+ or −) are present and are related by the $\left(\frac{2_1}{1}\right)$ superspace-group symmetry operator. These different chains run along a slice in the [101] direction and can be alternately denoted B+±, B±−, B−±, and B±+ (Figure 6). A relation can be established between the A and B chains: the disordered sites ± (labeled V(2)b and P(3)b, dark polyhedra in Figure 6) appear only in the B chains close to the A0 chains; the single sites (+ or −, labeled V(2)a and P(3)a, bright polyhedra in Figure 6) only appear close to the A1 chains. In fact, the average position of the O(6) atom in the A0 chain is compatible with the two enantiomorphic configurations of the "V(2)b−P(3)" chains, whereas the displaced O(6) position in the A1 chain is only compatible with one configuration in the adjacent B chain. These corner-sharing chains form bidimensional layers; the stacking of the chains A and B leads to a general alternation A1, B+±, A0, B±−, A1, B−±, A0, B±+, A1 (Figure 6), compatible with the $P2_1/c$ space group (Figure 4).

As a consequence, the ideal structure (Figure 6b) is related to that shown in Figure 6a by symmetrically replacing the "V(2)b−P(3)b" chains (dark polyhedra) with their enantiomorph. The disorder that appears in the layer is then easily explained by the random coexistence of the two enantiomorphic "V(2)b−P(3)b" chains within the same layer.

The coordination polyhedra of V(1), P(1), and P(2) remain relatively undistorted despite the modulation. This can be seen by examining the V(1)−O, P(1)−O, and P(2)−O distances (Table 3) and the O−O distances within each polyhedron. Consequently, the effect of displacive modulation on these polyhedra can be described as a combination of rotation and translation motions and weak distortion effects. The rotation and translation amplitudes were derived from a least-squares refinement assuming a rigid body model (Table 4). However this is not the case for the V(2) and P(3) polyhedra: large distortions arise because the displacement amplitudes of O(6) (V(2) polyhedron) and of O(7) (P(3) polyhedron) are large in comparison with the displacements of O(2) and O(4). Moreover, it should be noted that, in these polyhedra, split sites are involved, thus rendering a rigid body model meaningless.

5.4. An Explanation for the Low Intensity of Second Order Satellite Reflections. The electron diffraction study has shown the presence of second order satellite reflections of weak intensity, which were not measurable by X-ray diffraction. Their absence by XRD cannot by explained as a result of standard reflection conditions. An attempt at explaining their absence is given below.

Let us denote the distance between two split sites by $2\delta b$ and the contribution to the structure factor F_{hkl} of the corresponding atoms by $F_{1,hkl}$. Similarly, let us denote the modulated displacements along **b** by Δy_1 (Δy_2) in the unit cells $n_3 = 4n$ ($n_3 = 4n + 1$ respectively) and the contribution to the structure factor of the corresponding atoms by $F_{2,hkl}$. The variations δ with n_3 are very small, but the variations Δy_1 and Δy_2 are significant. The following results are found.

$$F_{1,hkl} = 2f_1\Big\{\cos 2\pi\alpha_1 \cos 2\pi k\delta \Big[1 + (-1)^l + 2(-1)^l \cos \pi\frac{l}{2}\Big] - \sin 2\pi\alpha_1 \sin 2\pi k\delta\,[1 - (-1)^l]\Big\}$$

with $\alpha_1 = hx_1 + lz_1 + k/4$ and f_1, the atomic scattering factor.

$$\begin{aligned} F_{2,hkl} = 2f_2\Big\{&\cos 2\pi\alpha_2 \cos 2\pi k\Delta y_1\,[1 + (-1)^l] \\ &- \sin 2\pi\alpha_2 \sin 2\pi k\Delta y_1\,[1 - (-1)^l] \\ &+ \cos 2\pi\alpha_2 \cos 2\pi k\Delta y_2\,[1 + (-1)^l] \cos \pi\frac{l}{2} \\ &- \sin 2\pi\alpha_2 \sin 2\pi k\Delta y_2\,[1 - (-1)^l] \cos \pi\frac{l}{2} \\ &- \cos 2\pi\alpha_2 \sin 2\pi k\Delta y_2\,[1 - (-1)^l] \sin \pi\frac{l}{2} \\ &- \sin 2\pi\alpha_2 \cos 2\pi k\Delta y_2\,[1 + (-1)^l] \sin \pi\frac{l}{2}\Big\} \end{aligned}$$

with $\alpha_2 = hx_2 + lz_2 + k/4$ and f_2, the atomic scattering factor.

If we consider the reflection class $h0l$, both $F_{1,h0l}$ and $F_{2,h0l}$ are equal to 0 for $l = 4n \pm 1$ and $l = 4n + 2$. The second-order satellites are then absent, as are first-order reflections. It should be noted that this extinction rule for $l = 4n + 2$ is not prescribed by the space group $P2_1/c$ but arises from the crystal structure when the displacive modulation of the split atoms and of the O(9) and O(10) atoms are neglected.

For the general reflections hkl, the structure factor expressions become

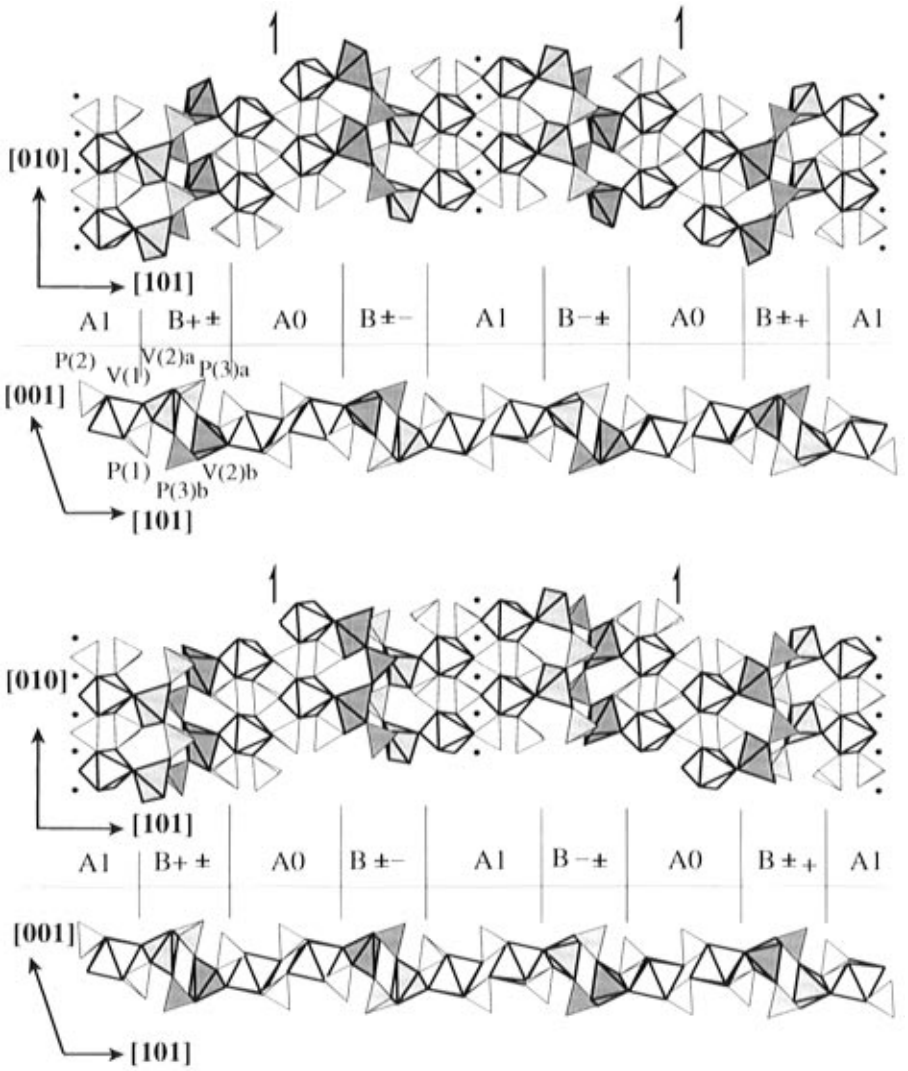

Figure 6. Schematic representation of a $[V_2P_3O_{13}]_\infty$ slice: blank polyhedra, displacively modulated coordination polyhedra of V(1), P(1), and P(2); gray polyhedra, disordered coordination polyhedra of V(2) and P(3); bright gray, V(2)a, P(3)a, full occupation (+ or −, see text); dark gray, V(2)b, P(3)b, disordered sites with occupation $^1/_2$. (a, top) The + configuration. (b, bottom) The − configuration.

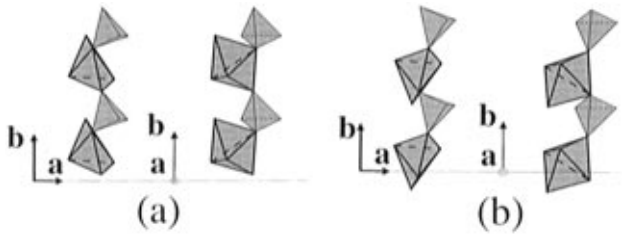

Figure 7. The two enantiomorphic configurations of the "V(2)b−P(3)b" chains in a projection perpendicular and parallel to the *x* axis: (a) the + configuration; (b) the − configuration.

$$F_{1,hkl} = -4f_1 \sin 2\pi\alpha_1 \sin 2\pi k\delta$$

$$F_{2,hkl} = -4f_2\left[\sin 2\pi\alpha_2 \sin 2\pi k\Delta y_1 + \cos 2\pi\alpha_2 \sin 2\pi k\Delta y_2 \sin \pi\frac{l}{2}\right]$$

for $l = 4n \pm 1$ (first-order satellites) and

$$F_{1,hkl} = 0$$

$$F_{2,hkl} = -8f_2 \cos 2\pi\alpha_2 \sin \pi k(\Delta y_1 + \Delta y_2) \sin \pi k(\Delta y_1 - \Delta y_2)$$

for $l = 4n + 2$ (second-order satellites).

Table 4. Rigid Body Displacements of the $P(1)O_4$, $P(2)O_4$, and $V(1)O_6$ Polyhedra[a]

		$n_3 = 2n$	$n_3 = 2n + 1$
tetrahedron $P(1)O_4$	T_y	−0.16	0.08
	R_x	7.5	5.5
	R_z	≃0	6.7
tetrahedron $P(2)O_4$	T_y	−0.06	0.13
	R_x	≃0	2.0
	R_z	≃0	5.8
octahedron $V(1)O_6$	T_y	−0.06	0.11
	R_x	−2.0	≃0
	R_z	−1.8	−4.5

[a] *T* and *R* stand for translation (Å) and rotation (deg), referring to the average structure, calculated in right-handed Cartesian axes with **i** and **j** parallel to **a** and **b** and $\mathbf{k} = \mathbf{i} \wedge \mathbf{j}$.

This result shows that only the atoms affected by the displacive modulation allow the existence of second order satellite reflections to be explained. It can be easily seen from the relations that their intensities are expected to be very weak in comparison with the first order satellite intensities.

6. Conclusion

Some original features can be outlined in the present structural study of the $Sr_2\ V_2O(PO_4)_3$ compound. A classical approach for the refinement of this structure proved to be unsuccessful for a number of reasons. These included the large size of the

unit cell, the low crystal symmetry ($P2_1/c$), the number of refinement parameters needed in this unit cell, and difficulties in locating most of the atoms with respect to the mirror plane *c*. This preliminary study indicated that most atoms were partially ordered over two sites. Nevertheless, because of the high quality of the crystal and the absence of significant diffuse scattering, the description of the crystal symmetry in this preliminary cell seemed to be inadequate. Close observation of reciprocal space allowed another interpretation of the crystal symmetry to be proposed. An abnormal reflection condition ($l \neq 4n + 2$) which is not explained in $P2_1/c$ was observed. The intensity ratios of these reflections suggested a superstructure with main and first-order satellites. Consequently, it was possible to perform a satisfactory refinement assuming a commensurately modulated structure, in the superspace group $P2_1/m(0,0,^1/_4)0s$.

Evidence for disorder was confirmed by the existence of split sites related by a mirror plane. However, this concerns only a few neighboring atoms in the structure. Chemical considerations indicate that this disorder corresponds to the random distribution of two enantiomorphic chains $[VPO_5]_\infty$ built up of corner-sharing VO_5 bipyramids and PO_4 tetrahedra running along **b**. Other atomic sites are related to the split sites by a superspace symmetry operator, but the phase of the modulation functions imposes either full or zero occupation for the new sites. This results in the alternation of two opposite configurations with 4-fold periodicity with respect to the **c′** subcell parameter. It is this very particular and original sequence of balanced symmetrical sites from one side of the mirror plane to the other which is responsible for the apparent absence of reflections with $l = 4n + 2$. Such an absence was also found for $KFeF_4$.[15] In neither case is it possible to speak of a rigorous extinction of some reflections. Their very weak measured intensity can be explained by the fact that the contribution of the displacive or occupational modulations to the intensity of these reflections, which can be considered only as second-order satellites according to the 4D symmetry, is very weak. As a consequence, these reflections are not measurable in standard diffraction conditions.

The other VO_6 and PO_4 coordination polyhedra are displacively modulated and can be described, in a first approximation, by translated and rotated rigid bodies. These displacements are closely related to the occurrence of the previously mentioned disorder. Two types of situations can occur: either (1) the shared atoms are almost in their average position and the adjacent polyhedra then have two equivalent possible configurations on one side or the other or (2) their displacement is at a maximum and only one of the two possible configurations is possible.

As a result of this study, an important point is to understand the local correlation between the enantiomorphic $[VPO_5]_\infty$ chains, which can occur both within the same layer and between adjacent layers. Unfortunately, the present diffraction data cannot give this answer. Further light may be shed on local correlations by electron diffraction and high-resolution electron microscopy analyses.

Acknowledgment. B. Domengès and J. Provost are gratefully acknowledged for carrying out electron microscropy analysis and magnetic measurements.

Supporting Information Available: Table S1, listing detailed crystallographic data, Table S2, giving anisotropic thermal parameters, and Table S3, listing atomic coordinates in the supercell (symmetry $P2_1/c$) (4 pages). Ordering information is given on any current masthead page.

IC970285P

(15) Sciau, Ph.; Grebille, D. *Phys. Rev. B* **1989**, *39*, 11982.